Casimir force between integrable and chaotic pistons

Ezequiel Álvarez[1], Francisco D. Mazzitelli[1], Alejandro G. Monastra[2], and Diego A. Wisniacki[1]
[1] *Departamento de Física, FCEyN UBA, and IFIBA, CONICET, Ciudad Universitaria, Pabellón I, 1428 Buenos Aires, Argentina and*
[2] *Gerencia de Investigación y Aplicaciones, Comisión Nacional de Energía Atómica, CONICET, Av. Gral. Paz 1499, 1650 San Martín, Argentina*

We have computed numerically the Casimir force between two identical pistons inside a very long cylinder, considering different shapes for the pistons. The pistons can be considered as quantum billiards, whose spectrum determines the vacuum force. The smooth part of the spectrum fixes the force at short distances, and depends only on geometric quantities like the area or perimeter of the piston. However, correcting terms to the force, coming from the oscillating part of the spectrum which is related to the classical dynamics of the billiard, are qualitatively different for classically integrable or chaotic systems. We have performed a detailed numerical analysis of the corresponding Casimir force for pistons with regular and chaotic classical dynamics. For a family of stadium billiards, we have found that the correcting part of the Casimir force presents a sudden change in the transition from regular to chaotic geometries.

I. INTRODUCTION

In the last years, there has been an increasing interest in the Casimir effect [1]. The Casimir force, which in its simplest version consists in the interaction between two perfectly conducting surfaces, involves the summation of the vacuum energy of the electromagnetic modes allowed by those surfaces, and therefore depends in a complex way on the spectrum associated to the considered geometry.

In this paper we will consider the following system: a pair of identical pistons of arbitrary shape separated by a distance a, contained in a very long cylinder with the same transversal shape [2]. All surfaces will be considered to be perfect conductors. This system has been solved, in the sense that there is an exact formula that relates the (renormalized) Casimir energy or force with the spectrum of the two-dimensional Laplacian operator constrained to the geometries that define the pistons [3]. The exact formula, first derived in [3] (see Eq. 5 below), involves a summation of functions of the eigenvalues of the two-dimensional Laplacian. This summation is different from the usual sum over modes that defines formally the vacuum energy, since the latter involves the eigenvalues of the three dimensional problem and gives a convergent result only after a proper subtraction. The (formal) sum over modes is not adequate to implement direct numerical evaluations of the Casimir energy even in the simplest situations [4], because of its highly oscillatory behavior. However, as we will see in many specific examples, this is not the case with the exact formula for pistons.

With the possibility to compute the Casimir force using the spectra of two-dimensional pistons, considered as quantum billiards, let us ask a natural question: is there any signature of the classical dynamics on the billiard in the Casimir effect? This conceptual question is based on the fact that spectra of chaotic and non-chaotic billiards are qualitatively different. Whereas the spectrum of a classically chaotic system shows level repulsion and its statistical properties are well described by Random Matrix Theory (RMT) [5], the energy levels of a regular classical system are Poisson distributed [6] (see [7] for a general discussion). Moreover, the spectrum of a given geometry can be written as the sum of a *smooth* plus an *oscillating* part. The smooth contribution to the spectrum depends only on geometric quantities like the area, perimeter, and the curvature of the border. But the oscillating part depends on quantities related to the classical periodic orbits of the system (as action, period and stability), which are completely different in the regular or chaotic case. Moreover, periodic orbits in regular systems come in continuous families, whereas in chaotic systems they are isolated. As already shown in Ref.[8, 9], the smooth part of the spectrum gives the short distance behavior of the force between pistons, the leading term being the well known Proximity Force Approximation (PFA). Therefore, any signal of quantum chaos, if present, should pop out in the difference between the full Casimir force and its smooth part.

The goal of this paper is to analyze the Casimir force between pistons trying to see some signature of chaos. For this reason we have computed the force between pistons of different shapes with regular and chaotic classical dynamics. In order to compute the Casimir force in our systems, it is necessary to handle summations of functions of the eigenvalues of the considered geometry. For very simple geometries, like a rectangle or equilateral triangle, the eigenvalues have explicit analytic expressions in terms of two quantum numbers, and the computation is relatively easy (although, as we will see, a large number of eigenvalues are necessary in order to reproduce the PFA limit).

For circles, the eigenvalues are defined as the zeros of Bessel functions. In this case, one can follow two different approaches: to compute numerically the eigenvalues, and then perform the summation, or, alternatively, to perform

the sum over the eigenvalues by using the argument theorem.

Besides, for rectangular and equilateral triangular billiards, the correcting part of the Casimir force, that comes from the oscillating part of the spectrum, can be computed using exacts results from semiclassical periodic orbit theory [10]. We remark that semiclassical techniques have been already used in the computation of Casimir force [11]. For more complex geometries, semiclassical theory is only approximated and the effort to compute the periodic orbits is enormous. The only alternative is to find the eigenvalues associated to a given geometry using sophisticated methods. We will show that, with some computational effort, the exact formula is useful to evaluate the Casimir interaction between pistons for both integrable and non-integrable geometries.

The paper is organized as follows. In Section II we review the main results for the force between pistons. We include a discussion of the exact formula, the behavior of the Casimir energy at large distance, and the relation between the short distance behavior and the smooth part of the spectrum. In Section III we compute the Casimir force between pistons with integrable classical dynamics. We will consider rectangular, triangular and circular pistons. We will use the large and short distance behaviors as benchmarks for the numerical calculations, and show that, up to a given accuracy, it is possible to find analytic expressions for the force for any distance between the pistons. We will also compute the correcting part of the force, and find that circular pistons have a different behavior in the short distance limit: the leading contribution to the correcting part of the force is finite for triangles and rectangles, and diverges for circles. In Section IV we present the results for the force between pistons that are billiards with chaotic classical dynamics. The calculation of the Casimir force in this case was done by computing the corresponding eigenvalues through the *scaling method* [12]. In particular, we will analyze a family of stadium billiards, and the uniformly hyperbolic Sinai-type billiard introduced in Ref.[13]. For each considered geometry, we will compute the full Casimir force, paying particular attention to its correcting part. We will show that at short distances all geometries with curved boundaries present a similar divergent behavior. Section V contains an analysis of the Casimir force associated to the oscillating part of the spectrum for both integrable and chaotic pistons. The analysis is based on the computation of the correcting part of the force for a family of billiards that interpolates between a regular geometry (quarter of circle) and chaotic billiards. We will see that, in the short distance limit, the correcting part of the force has an abrupt change in the transition from the quarter of circle to a stadium billiard. We present our conclusions in Section VI.

II. CASIMIR FORCE BETWEEN PISTONS: THE EXACT FORMULA

We consider a very long electromagnetic cylindrical cavity, with an arbitrary section (which we will assume to be simply connected). The cavity contains two plates (pistons) separated by a distance a. All surfaces are perfectly conducting. The $\mathbf{z}$-direction is the axis of the cavity, and we will denote by $\mathbf{x}_\perp$ the coordinates in the transverse sections. At classical level, the electromagnetic field admits a description in terms of independent Transverse Electric (TE) and Transverse Magnetic (TM) modes, which are defined with respect to $\mathbf{z}$-direction. This is possible due to the particular geometry we are considering, that have an invariant section along the $\mathbf{z}$ axis. As the section is simply connected, there are no Transverse Electromagnetic Modes (TEM). The relevance of TEM modes in the Casimir force between pistons with non-simply connected sections has been analyzed in Ref.[14].

As discussed in Ref.[14], TE and TM Casimir energies correspond to that of a set of massive scalar fields in $1+1$ dimensions, with masses given by the eigenvalues associated to the two-dimensional pistons, that we will denote by $\lambda_{k\mathrm{N}}$ and $\lambda_{k\mathrm{D}}$. More explicitly, the eigenfrequencies associated to the TE and TM modes are

$$\begin{aligned} w_{k,n}^{\mathrm{TE}} &= \sqrt{(\tfrac{n\pi}{a})^2+\lambda_{kN}^2} \quad (n=1,2,3,..) \\ w_{k,n}^{\mathrm{TM}} &= \sqrt{(\tfrac{n\pi}{a})^2+\lambda_{kD}^2} \quad (n=0,1,2,...), \end{aligned} \tag{1}$$

where the eigenvalues are defined by

$$\nabla_\perp^2 \varphi_{\mathrm{TE,TM}} = -\lambda_{\mathrm{N,D}}^2 \varphi_{\mathrm{TE,TM}} \,. \tag{2}$$

The eigenfunctions $\varphi_{\mathrm{TE,TM}}$ satisfy Neumann and Dirichlet boundary conditions, respectively, on the border of the transversal section. The $\varphi_{\mathrm{TE}} = const$ eigenfunction with $\lambda_{\mathrm{N}} = 0$ should be excluded because it does not correspond to a physical electromagnetic solution.

The Casimir energy E_m and force F_m for a field of mass m in $1+1$ dimensions has been computed previously by many authors [15]. They are given by

$$E_m(a) = -\frac{1}{2\pi}\sum_{l=1}^{+\infty}\frac{mK_1(2lma)}{l}\,, \tag{3}$$

and

$$F_m(a) = -\frac{\partial E_m}{\partial a} = \frac{1}{\pi}\sum_{l=1}^{+\infty} m^2 K_1'(2lma)\,, \tag{4}$$

where K_1 is the modified Bessel function of the second kind and the prime denotes derivative with respect to the argument. Using these results and the analogy between the TE and TM eigenfrequencies with the eigenfrequencies of massive scalar fields in $1+1$ dimensions, we can easily obtain the TE and TM contributions to the Casimir force between pistons in the cylindrical cavity

$$F^{\rm TE}(a) + F^{\rm TM}(a) = \frac{1}{\pi}\sum_{l=1}^{+\infty}\left(\sum_{\lambda_{k\rm N}} \lambda_{k\rm N}^2 K_1'(2l\lambda_{k\rm N}a) + \sum_{\lambda_{k\rm D}} \lambda_{k\rm D}^2 K_1'(2l\lambda_{k\rm D}a)\right)\,. \tag{5}$$

This equation has been previously obtained in Ref. [3] using a different method. We stress that the formula is valid for a cavity of arbitrary section. In the rest of the paper we will be mainly concerned with the particular case of Dirichlet boundary conditions (which correspond to TM modes), because this will be enough for our purposes. Therefore we will omit the subindex D in the eigenvalues and the supraindex TM in the forces.

In the next sections we will present numerical evaluations of the Casimir force between pistons using Eq. 5. In the cases where the eigenvalues are known analytically or numerically, the evaluation will be performed by computing explicitly the summations over l and λ_k in Eq. 5. There are some cases where the eigenvalues associated to a given geometry are known implicitly through the zeros of a function $f(\lambda) = 0$. In this case, the sum over eigenvalues can be performed using the argument theorem

$$\sum_{\lambda_k} \lambda_k^2 K_1'(2l\lambda_k a) = 2\pi i \oint_C dz\, z^2 K_1'(2zla)\frac{f'(z)}{f(z)}\,, \tag{6}$$

where the integral is performed in the complex plane z along a closed contour C that encloses all zeros of $f(z)$.

We will now describe some general properties of the force between pistons given in Eq. 5. The function

$$K_1'(x) = -\frac{1}{2}(K_0(x) + K_1(x))$$

is a negative and increasing function for real and positive arguments, and vanishes exponentially for $x \to \infty$. Therefore, the force between pistons is always attractive and decreases with distance. Moreover, at large distances, the sum is dominated by the term with the lowest eigenvalue λ_1 and $l = 1$, that is

$$F(a) \approx F_\infty(a) = -\frac{1}{2\pi}\lambda_1^2\left(K_0(2\lambda_1 a) + K_1(2\lambda_1 a)\right) \approx -\frac{1}{2}\left(\frac{\lambda_1^3}{\pi a}\right)^{1/2} e^{-2\lambda_1 a}\,. \tag{7}$$

The exponential behavior is due to the finite size of the pistons, that produce a gap in the spectrum. The above approximation is valid as long as $a\lambda_1 \gg 1$.

The behavior at short distances requires a deeper analysis. As the distance between pistons decreases, more and more eigenvalues give a sizable contribution to the force. Taking into account the exponential behavior of the Bessel functions, if in the numerical computation one neglects terms that are smaller than e^{-D} for a given accuracy, all terms with $2l\lambda_k a_{min} < D$ should be kept in the calculation, where a_{min} is the minimum distance for which the force is numerically computed.

It is useful to rewrite Eq. 5 in an integral form

$$F(a) = \frac{1}{\pi}\sum_{l=1}^{\infty}\int {\rm d}\epsilon\ \epsilon\ K_1'(2la\sqrt{\epsilon})\rho(\epsilon)\ , \tag{8}$$

where $\rho(\epsilon) = \sum_k \delta(\epsilon - \lambda_k^2) = \frac{{\rm d}N}{{\rm d}\epsilon}$ is the density of states (or energy levels). The number of energy levels N below a given energy ϵ can be approximated using the so called Weyl's theorem [7], which for two dimensional billiards with Dirichlet boundary conditions gives

$$N(\epsilon) = \left(\frac{A}{4\pi}\epsilon - \frac{P}{4\pi}\epsilon^{1/2} + \chi\right)\Theta(\epsilon) + \widetilde{N}(\epsilon)\,, \tag{9}$$

where A is the area of the piston, P its perimeter, and χ is related to the shape of the boundary through

$$\chi = \frac{1}{24}\sum_i \left(\frac{\pi}{\alpha_i} - \frac{\alpha_i}{\pi}\right) + \frac{1}{12\pi}\sum_j \int_{\gamma_j} \kappa(\gamma_j) d\gamma_j \, . \tag{10}$$

Here α_i is the interior angle of each corner and $\kappa(\gamma_j)$ is the curvature of each smooth section γ_j of the border. The term $\widetilde{N}(\epsilon)$ contains lower order contributions that vanish in the limit $\epsilon \to \infty$. It oscillates rapidly with energy, and is related with the classical periodic orbits of the billiard. (For TE modes the sign of the perimeter term changes and the factor χ should be replaced by $\chi - 1$ in Eq. 9).

Introducing the first three terms of the Weyl expansion into Eq. 8, the integral and the infinite sum over l can be solved, giving

$$F(a) \approx F_W(a) = -\frac{3\zeta(4)}{8\pi^2 a^4} A + \frac{\zeta(3)}{32\pi a^3} P - \frac{\zeta(2)\chi}{4\pi a^2} \, . \tag{11}$$

This result has already been shown, using different methods, in Refs. [3, 8, 9]. The first term is the usual PFA proportional to the area. There are also corrections of lower order on a related to the perimeter and curvature of the boundary of the billiard, although the regular or chaotic classical dynamics on the surface does not enter in this expression.

III. PISTONS WITH REGULAR CLASSICAL DYNAMICS

In this Section we use the above results in order to compute numerically the Casimir force between pistons with rectangular, triangular and circular shapes. Thinking these shapes as billiards, they all have regular dynamics as they have two constants of motion (as required for two dimensional systems). We verify that the results converge to the expected F_W expression Eq. 11 for short distances and to the F_∞ expression, Eq. 7, for large distances.

In order to compute the Casimir force from Eq. 5, it is necessary to obtain the eigenvalues of the Laplace equation for each geometry. For a rectangular piston of sides L_x and L_y, these eigenvalues are trivially

$$\lambda_{nm} = \sqrt{\left(\frac{\pi n}{L_x}\right)^2 + \left(\frac{\pi m}{L_y}\right)^2} \tag{12}$$

with indices $n, m \geq 1$ for Dirichlet boundary conditions (TM modes). For Neumann boundary conditions (TE modes) one of the indices can be zero (but not both at the same time).

For an equilateral triangle of side L

$$\lambda_{nm} = \frac{4\pi}{3L}\sqrt{n^2 + m^2 - n\,m} \tag{13}$$

with $n \geq 1$ and $m \geq n+1$ for Dirichlet boundary conditions, and $n \geq 0$ and $m \geq n$ for Neumann boundary conditions, excluding the term $(n, m) = (0, 0)$, see [10, 16] for further details about the equilateral triangular billiard.

On the other hand, for a circular piston of radius R, the eigenvalues of the Laplace equation are given implicitly as the solutions of

$$\text{Dirichlet b.c.} \;\rightarrow\; J_n(R\,\lambda_{nm}) = 0, \tag{14}$$

$$\text{Neumann b.c.} \;\rightarrow\; J_n'(R\,\lambda_{nm}) = 0, \tag{15}$$

where $n \geq 0$ is an integer which labels the order of the Bessel function, and m refers to its m-th root. For $n = 0$, the eigenvalues are non degenerated, and for $n \geq 1$ they are double degenerated. For Neumann boundary conditions the first trivial zero of J_0', that is $\lambda_{01} = 0$, is excluded. Therefore, the Casimir force can be computed using Cauchy's theorem as in Eq. 6. Alternatively, the eigenvalues can be computed numerically from Eq. 14, and then use Eq. 5 to calculate the force. We have used both methods (see appendix A for details on the samples of used eigenvalues).

A. Casimir force

We have computed numerically the Casimir force $F(a)$ for the three regular pistons and compared it to the predicted behavior for short piston separation, $F_W(a)$, and long separation, $F_\infty(a)$. The criterion to define whether a separation is long or short depends on the value of a compared to the characteristic lengths of each shape. Since the result for all shapes are qualitatively the same, we have only plotted the results of this comparison for the square with area $A = 1$ in Fig. 1. (Observe that setting the area to unity is equivalent to use units of $\sqrt{area}$ for the distance a and $1/area$ for the resulting Casimir force. All figures and results in this paper are to be understood in these units.) As it can be seen in the short-distance region the convergence improves as we include each term of the Weyl expression Eq. 11. On the other hand, in the large-distance region, we verify the convergence to the expression in Eq. 7 which is a function of the smallest eigenvalue. Moreover, in this region we have also plotted the next-to-leading order large distance asymptotic expression (including the first two eigenvalues) to show explicitly that it is possible –and simple– to obtain, by choosing different approximations in each region, an analytic approximation of the Casimir force which agrees within a given accuracy with the numerical result. Indeed, adding a few additional terms in the large distance expansion is possible to describe the numerical results with analytic approximations within a 1% for any value of a.

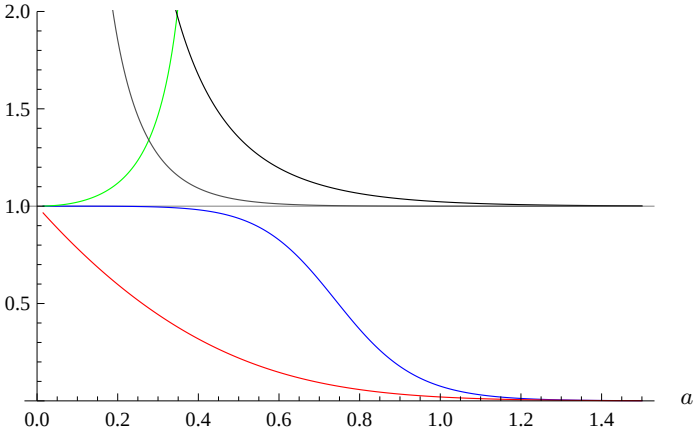

FIG. 1: (Color online) Ratio of the numeric Casimir force between squared-shape pistons to the Weyl expression (Eq. 11), F_{num}/F_W, and to the large distance asymptotic expression (Eq. 7), F_{num}/F_∞. For those converging to 1 at small a, from bottom to top corresponds to the leading (red), next-to-next-to-leading (blue) and next-to-leading order (green) in F_W (Eq. 11), respectively. For those converging to 1 at large a, from top to bottom corresponds to the ratio of the numeric force to the large-distance expression (black) Eq. 7 and to the next-to-leading order asymptotic expression (grey) –id est, including the two first eigenvalues. All others shapes (rectangle, triangle, circular and also the non-integrable shapes discussed in next Section) behave qualitatively the same.

In order to compare the Casimir force for the integrable pistons we have plotted in Figure 2 the numeric Casimir force for the different geometries while keeping constant the area $A = 1$ for all shapes. Given the short-distance expression $F_W(a)$ we find that the differences between the forces at short distances must come from the different perimeters of the pistons. Whereas in the large-distance region the difference must come from the first eigenvalue λ_1 (see Eq. 7). In table of Figure 2 we give the perimeter and first eigenvalue for the geometries under study, as well as the geometrical χ factor. As it can be seen, there is no cross-over of the lines in Figure 2 from large to short distances. However this is not a general property, since it exists a *spectral theory* theorem that states that if region R contains region R' then the lowest eigenvalue of the Laplacian operator restricted to Dirichlet boundary conditions on R is smaller than the lowest eigenvalue of R' [17]. Therefore, it is possible to imagine pistons A and B where A is contained in B, but A has a larger perimeter and, therefore, the ordering in the Casimir forces for short-distances is the contrary to the one for large-distances. We will see an explicit example in Section IV. Another interesting property is that, among all possible two-dimensional shapes with a given area, the circle has the lowest first eigenvalue [17]. Therefore, at large distances the interaction between circular pistons is stronger than for pistons of any other shape.

We end this Section with some comments on Neumann boundary conditions (TE modes) concerning the pistons studied in this Section. We have computed the Casimir force in each shape for TE modes. The ordering of the results for small and large distances is the opposite than for Dirichlet boundary conditions (TM modes). At short distances this follows from the expression of F_W: as already mentioned after equation Eq. 11, the term proportional to the perimeter changes sign for Neumann boundary conditions. On the other hand, at large distances the opposite order comes from the relative values of the first eigenvalue of each geometry. The first eigenvalue of the billiards considered

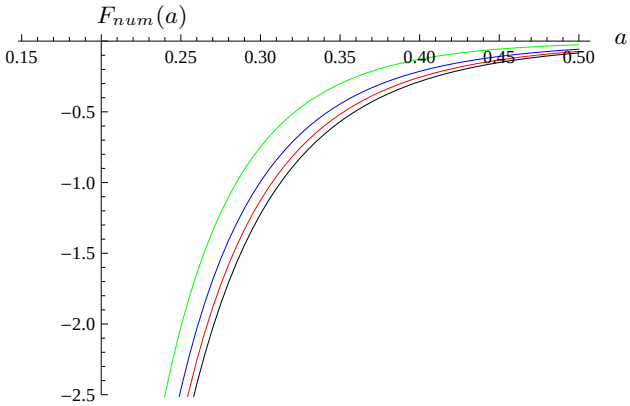

shape	P	χ	λ_1
circle	3.54	0.16	4.26
square	4	0.25	4.44
triangle	4.56	0.33	4.77
rectangle 4:1	5	0.25	6.47

FIG. 2: (Color online) Casimir force between integrable-shaped pistons with area equal to unity. The ordering for small and large a may be understood from the corresponding asymptotic expressions in Eq. 11 and Eq. 7, respectively, as a function of the ordering in the perimeter and first eigenvalue for each geometry. From top to bottom the lines correspond to a $4:1$ rectangle (green), an equilateral triangle (blue), a square (red) and a circle (black), respectively. The table shows the different parameters of each geometry that enter into Eq. 11 and Eq. 7.

here, for Neumann boundary conditions, is always smaller than the first one for Dirichlet boundary conditions. Therefore the force decreases more slowly as $a \to \infty$.

B. Correcting part of the force

To analyze the effects of the classical dynamics on the Casimir force we should investigate the difference

$$\delta F(a) = F(a) - F_W(a)\,, \tag{16}$$

since the Weyl terms F_W only depends on geometrical quantities. The difference δF is related to the oscillating part of the spectrum and will contain information of classical periodic orbits. From Eq. 11, where the last term proportional to χ goes as a^{-2}, we typically expect that

$$\lim_{a\to 0} a^2 \delta F(a) = 0. \tag{17}$$

To see if there is a qualitatively different behavior as $a \to 0$ for different type of dynamics, we study numerically the difference of the force for regular as well as for chaotic (next Section) geometries.

We have plotted δF for the integrable shapes studied in Figure 3. As it can be seen, the geometries consisting only in straight lines and angles (square, rectangle and triangle) reach a constant for short distances. For these geometries, semiclassical expansion can be done in an exact way, and the short distance behavior can be obtained explicitly in terms of periodic orbits (see Appendix B). The constant can be precisely computed and as it can be seen in the Figure (dashed asymptotes) matches perfectly with the numerical evaluation of δF. On the other hand, the circle shows a divergence in δF for $a \to 0$. Based on the examples studied in next sections we would conjecture that this is a general property for billiards with curved boundaries.

It is worth mentioning that, had we forgotten to sum a single eigenvalue in Eq. 5 of those required by the accuracy sought (see discussion after Eq. 7), then the condition Eq. 17 would be violated. Indeed, the contribution of a given eigenvalue λ_k to the force is

$$F_k(a) = \frac{1}{\pi} \sum_{l=1}^{+\infty} \lambda_k^2 K_1'(2l\lambda_k a)\,, \tag{18}$$

and a simple numerical analysis shows that F_k diverges as $1/a^2$ for $a \to 0$. Therefore the wrongly-computed $\delta F(a)$ would diverge as $1/a^2$ violating Eq. 17. We have verified that this is not the case for all the numerical calculations.

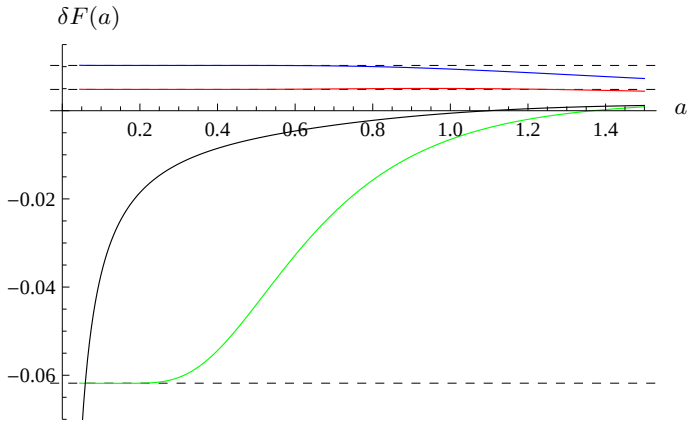

FIG. 3: (Color online) Correcting part of the force ($\delta F = F - F_W$) for integrable geometries. Solid lines from top to bottom at $a = 1$ correspond to triangle (blue), square (red), circle (black) and rectangle 4:1 (green), respectively. The dashed lines are the asymptotes to which the polygon geometries converge according to the explicit calculations in Appendix B.

IV. PISTONS WITH CHAOTIC CLASSICAL DYNAMICS

In this Section we compute the Casimir force between pistons with non-integrable shapes. We study a family of stadiums billiards and a Sinai-type billiard. A stadium consist of a rectangle of sides r and ℓ with a quarter of circle of radius r, as shown in Figure 4. It has been shown that the classical motion of a particle inside a stadium is fully chaotic [18]. The second kind of chaotic billiard is also shown in Figure 4. It has been extensively studied in Ref. [13], and its eigenvalues have been computed [19].

The computation of the Casimir force requires the knowledge of the eigenvalues of the Laplace operator with a given boundary condition. The eigenvalues of the chaotic billiards were computed using the scaling method [12]. This powerful method was proposed by Saraceno and Vergini and up to date is one of the most efficients methods to solve the Helmholtz eigenvalue problem in a hard-walled billiard (with Dirichlet boundary conditions). Using this method it is possible to find all eigenvalues and eigenfunctions in a narrow energy range by solving a generalized eigenvalue problem in terms of quantities over the boundary of the cavity. The gain being that in a single computational step a number of accurate eigenvalues are obtained in a constant proportion to the dimension of the matrices scaling as $\mathcal{O}(k)$ where $k = 2\pi/\lambda$ is a referential wave-number. The success of the method is essentially based on the fact that eigenstates are quasi-orthogonal on the boundary. The scaling method was used to numerically compute extremely high-lying energy levels of $2D$ and $3D$ billiards [20, 21].

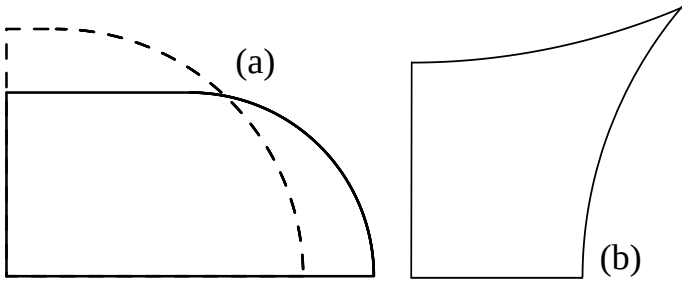

FIG. 4: Shape of chaotic billiards pistons used in the calculations. (a) Stadiums are a family of figures formed by the union of a rectangle (of sides r and ℓ) and a quarter of circle (of radius r); once the area is fixed to unity they are labeled by the ratio ℓ/r. In the Figure we show a stadium with $\ell/r = 1$ (solid) and $\ell/r = 0.2$ (dashed). (b) Uniformly hyperbolic Sinai-type chaotic billiard, also used in this work with area fixed to unity (see [13] for details).

A. Casimir force

We have computed the Casimir force between stadium pistons with Dirichlet boundary conditions for $\ell/r =$ 1, 0.705, 0.7, 0.205, 0.2, 0.005 and 0, as well as for the Sinai-type billiard, all with area $A = 1$ (see Appendix A for the details in the samples of eigenvalues).

We have verified the correct convergence of the numerical computation to the expected short and long distance behavior using Eq. 11 and Eq. 7, respectively, for all billiards.

We present in Figure 5 the numeric Casimir force for three relevant shapes. At this level there are no qualitative differences with the force of integrable geometries. However, in this case, we do see a cross-over of the forces between the Sinai-type piston and the stadiums, since the ordering in the perimeter (see table in Figure 5) is contrary to the order in the first eigenvalue and, therefore, the ordering for the asymptotic small and large distance is reversed (see discussion in previous Section).

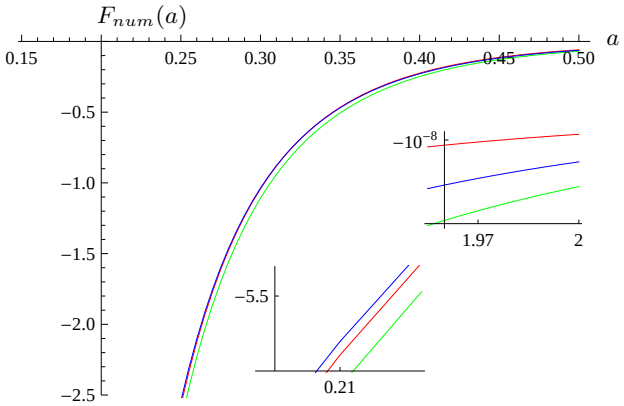

shape	P	χ	λ_1
stadium $\ell/r = 1$	4.16	0.23	4.86
stadium $\ell/r = 0.2$	4.00	0.23	4.68
Sinai-type billiard	4.52	0.43	4.64

FIG. 5: (Color online) Casimir force for different shaped chaotic pistons. For small a (lower inset) from top to bottom: Sinai-type billiard (blue), stadium $\ell/r = 1$ (red) and stadium $\ell/r = 0.2$ (green). For large a (upper inset) from top to bottom: stadium $\ell/r = 1$ (red), Sinai-type billiard (blue), and stadium $\ell/r = 0.2$ (green). Due to the relationship between the perimeters and the first eigenvalue there is cross-over of the forces from the small to the large distance regime. At distances larger than those plotted in this figure there is a crossover between the green and blue curves, as expected from the fact that the lowest eigenvalue of the $\ell/r = 0.2$ stadium is slightly larger than the one of the Sinai-type billiard.

B. Correcting part of the force

In this Section we investigate the correcting part of the Casimir force that comes from the oscillating part of the spectrum for the non-integrable geometries under study. In all cases we found that in the limit of short distances $\lim_{a\to 0} \delta F(a) = \pm\infty$. This is contrary to the the straight-line-contours integrable pistons (rectangles and equilateral triangle), but similar to the curved-line-contour (circle). Moreover, as in the circle, for these chaotic pistons with curved contours $\delta F \sim 1/a$ as $a \to 0$, because it is observed that $\lim_{a\to 0} a\delta F(a) =$ constant. These results are plotted in Figure 6. In virtue of the discussion in the previous Section, we verified that $a^2\delta F(a) \to 0$ as $a \to 0$, and therefore we have not omitted any relevant eigenvalue.

V. CHAOTIC TRANSITION STUDY

In order to look for chaotic distinctive signals we have studied $F(a)$ and $\delta F(a)$ in a transition between chaotic to regular geometries. These correspond to the maximal-chaotic $\ell/r = 1$ stadium to the non-chaotic $\ell/r = 0$ stadium, which corresponds to the quarter of circle. In this transition, for reasons that will became clear below, we have stepped in the $\ell/r = 1,\ 0.705,\ 0.7,\ 0.205,\ 0.2,\ 0.005$ and $\ell/r = 0$ (quarter of circle) stadiums.

In a first stage we have computed numerically $F(a)$ and, as expected, we have found no differences in these geometries that could come from a chaotic versus non-chaotic behavior. This would have been the case if the $\ell/r = 0$ stadium (quarter of circle) would have had a distinctive behavior in relation to the others $\ell/r \neq 0$ stadiums. We have plotted $F_{num}(a)$ for some relevant stadiums in Figure 7. For small a, we have that since all stadiums have the same

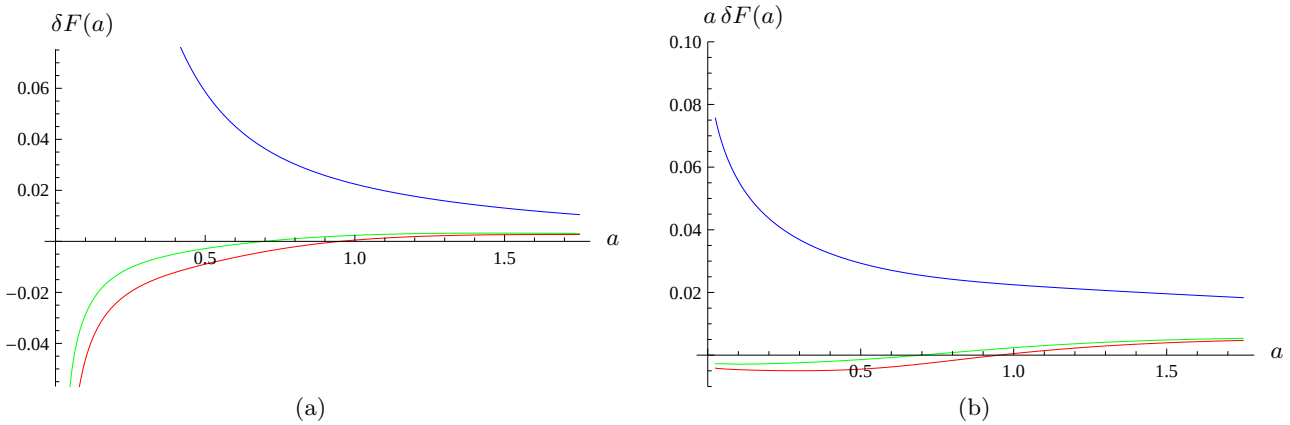

FIG. 6: (Color online) (a) Correcting part of the Casimir force for chaotic geometries, all diverge as $a \to 0$. (b) $a\,\delta F(a)$ for these same geometries. We find that all converge to a constant. On both figures, from top to bottom the plots correspond to the Sinai-type billiard (blue), the stadium $\ell/r = 0.2$ (green) and the stadium $\ell/r = 1$ (red), respectively.

area and geometrical χ-factor, $F_{num}(a)$ is ruled by the perimeter term in $F_W(a)$ (Eq. 11). It is interesting to notice that, for fixed area, the perimeter as a function of ℓ/r is not a monotone function but, instead, it has a minimum at $\ell/r = 1 - \pi/4 \approx 0.21$. This ordering in the perimeter of the stadiums is also observed in $\delta F(a)$ for large a.

On the other hand, the study of $\delta F(a)$ has shown a qualitative separation between the chaotic stadiums and the non-chaotic $\ell/r = 0$ quarter of circle. Since the expected differences should show up for small a and $\delta F(a)$ diverges as $a \to 0$ we found suitable to study this qualitative behavior in the product $a\,\delta F(a)$ where we avoid the divergence. We have found that a small variation of ℓ/r produces a small variation of $a\,\delta F(a)$ for $\ell/r \not\approx 0$. On the other hand, for $\ell/r \approx 0$ we have found that $a\,\delta F(a)$ is very sensitive to ℓ/r. To show this behavior we have plotted in Figure 8 the product $a\,\delta F(a)$ for three characteristic values of ℓ/r and a tiny variation on each of them. As it can be seen in the figure, the plots for $\ell/r \not\approx 0$ ($\ell/r = 0.2,\ 0.205,\ 0.7$ and 0.705) show practically no difference, whereas the plots for $\ell/r = 0$ and $\ell/r = 0.005$ show a large variation. In other words, the function $U(\ell/r) = \lim_{a\to 0} a\,\delta F(a)$ has a smooth behavior at $\ell/r \neq 0$, and a sudden change at $\ell/r = 0$.

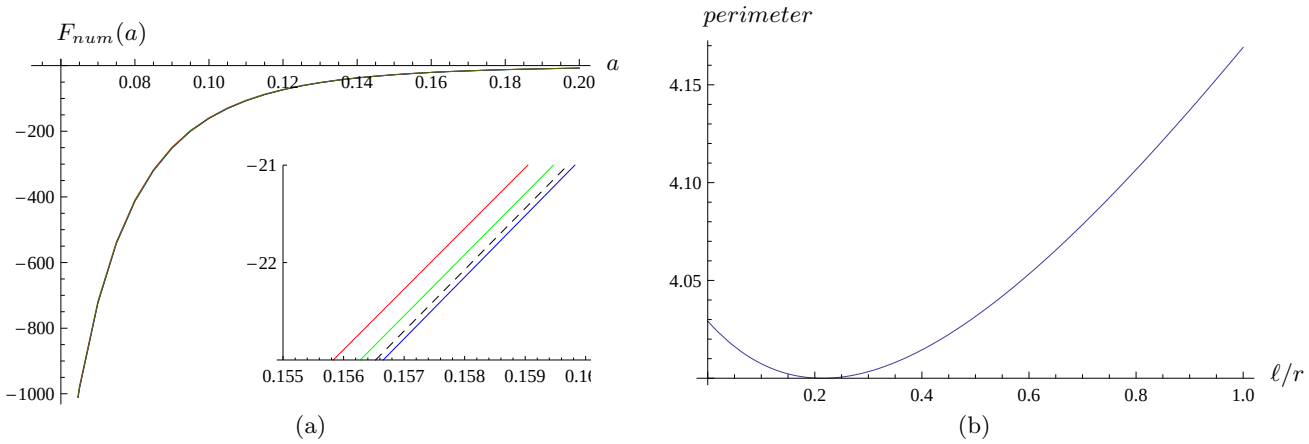

FIG. 7: (a) (Color online) Numeric Casimir force for several stadiums. The lines correspond from top to bottom to stadiums with $\ell/r = 1$ (red), 0.7 (green), 0 (black dashed) and 0.2 (blue), respectively. (b) Perimeter of a stadium of area equal to 1 as a function of ℓ/r. Observe the correlation between both figures, since the perimeter rules the force ordering for the equal-area stadiums.

VI. FINAL REMARKS

In this work we have studied numerically the Casimir force between two identical pistons of several shapes inside a cylindrical cavity. We summarize our main results and conclusions.

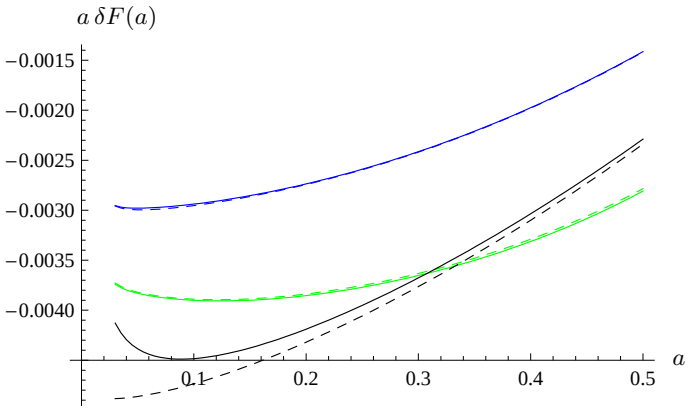

FIG. 8: (Color online) $a\,\delta F(a)$ for different values of ℓ/r and a tiny variation on it. From top to bottom: 0.205 (blue), 0.2 (blue dashed), $\ell/r = 0.705$ (green), 0.7 (green dashed), 0.005 (black) and 0 (black dashed). The plot shows the sensitivity of $\delta F(a)$ in ℓ/r at $\ell/r \approx 0$, where the transition from non-chaotic to chaotic occurs.

We have presented explicit numerical calculations for the force between pistons of different shapes. The numerical calculations were verified using the large and small distance behaviors, which are known analytically. Moreover, we have shown that it is easy to obtain accurate analytic expressions for the force in the whole range of distances.

For the simplest geometries (rectangles and triangles), the eigenvalues are known analytically, and the evaluation of the force is relatively simple. For the case of the circle, the eigenvalues are known implicitly, and we used two different methods to compute the sum over eigenvalues: Cauchy's theorem and a numerical evaluation of the eigenvalues. Finally, for the more complex geometries, the only alternative is to compute the eigenvalues numerically and then use the exact formula for the force. The evaluation of the force at short distances involves a very large number of eigenvalues, and therefore a precise and efficient method to compute thousands of eigenvalues is necessary. We have used a particular method developed in the context of quantum billiards. At this point we would like to stress that the combination of this or alternative methods to compute eigenvalues [22] with Cauchy's theorem could be particularly useful to compute the Casimir energy for other geometries (see for instance [23]).

One of the original motivations of this work was to look for signals of quantum chaos in the Casimir force for the piston geometry. For this reason, we evaluated the part of the force originated by the oscillating part of the spectrum. On the one hand, we have seen a set-apart behavior depending on whether the boundary of the piston contains curved-lines or not. In the first case δF diverges as $a \to 0$, while in the second case converges. A more detailed analysis of the transition between chaotic and regular geometries shows a different behavior for the non-chaotic geometry in the part of the force coming from the oscillatory part of the spectrum, more explicitly in the finite limit $U = \lim_{a\to 0} a\,\delta F(a)$. We analyzed a one parameter (ℓ/r) family of stadiums, that starts with an integrable geometry (a quarter of circle, $\ell/r = 0$). The finite limit is a function of this parameter, $U = U(\ell/r)$ that has a smooth behavior for $\ell/r \neq 0$, and a jolt at $\ell/r = 0$.

In this paper we analyzed the eventual existence of footprints of the statistical properties of the spectrum in the Casimir force. There could be signals of quantum chaos in the fluctuations of the Casimir force. We hope to address this interesting problem in a forthcoming publication.

This work has many numerical results which have given us clues on the behavior of the Casimir Force for different shapes of the pistons. It would be very interesting to explore and verify analytically these results.

Appendix A: Eigenvalues samples

For the different shaped pistons we have used different set of eigenvalues. The following table summarizes the required information to reproduce our results.

shape	total eigenvalues	maximum eigenvalue
square	30000	615.95
rectangle 4:1	30000	616.45
triangle	61075	963.35
circle	19984	549.38
1/4–circle	16111	451.95
stadium $\ell/r = 1$	17247	467.59
stadium $\ell/r = 0.705$	17254	467.7
stadium $\ell/r = 0.7$	21439	521.08
stadium $\ell/r = 0.205$	17258	467.67
stadium $\ell/r = 0.2$	18000	477.58
stadium $\ell/r = 0.005$	17257	467.63
Sinai-type billiard	62076	885.47

Appendix B: Correcting part of the force for rectangles and triangles

As expression (5) for the Casimir force, the Casimir energy can be rewritten in an integral form

$$E^{TM}(a) + E^{TE}(a) = -\frac{1}{2\pi}\sum_{l=1}^{\infty}\frac{1}{l}\int \mathrm{d}\epsilon\sqrt{\epsilon}K_1(2la\sqrt{\epsilon})[\rho_{\mathrm{D}}(\epsilon) + \rho_{\mathrm{N}}(\epsilon)] \ , \tag{B1}$$

where

$$\rho_{\mathrm{D,N}}(\epsilon) = \sum_k \delta(\epsilon - \lambda^2_{k\mathrm{D,N}}) = \bar{\rho}_{\mathrm{D,N}}(\epsilon) + \widetilde{\rho}_{\mathrm{D,N}}(\epsilon) \tag{B2}$$

is the density of states with Dirichlet (Neumann) boundary conditions, and where we have already split the density into a Weyl smooth part plus an oscillating part. For both rectangular and equilateral triangular billiards, there are explicit exact formulas for this semiclassical expansion using Poisson summation formula from explicit expressions (12) and (13) for the eigenvalues (see [16] for details). The smooth part has the usual form for 2D billiards

$$\bar{\rho}_{\mathrm{D,N}}(\epsilon) = \frac{A}{4\pi} \mp \frac{P}{8\pi\sqrt{\epsilon}} + \chi_{\mathrm{D,N}}\delta(\epsilon) \tag{B3}$$

where $A = L_xL_y, P = 2(L_x + L_y), \chi_{\mathrm{D}} = 1/4, \chi_{\mathrm{N}} = -3/4$ for rectangular billiard of sides L_x and L_y, and $A = \sqrt{3}L^2/4, P = 3L, \chi_{\mathrm{D}} = 1/3, \chi_{\mathrm{N}} = -2/3$ for equilateral triangular billiard of side L. The contribution of this smooth part of the Weyl series to the Casimir energy can be evaluated analytically, giving an exact result that has already been discussed, see Eq. 11.

The oscillating parts have the following exact expressions in terms of periodic orbits

$$\text{rectangle} \to \widetilde{\rho}_{\mathrm{D,N}}(\epsilon) \ = \ \frac{A}{4\pi}\sum_{\mathbf{M}} J_0(L_{\mathbf{M}}\sqrt{\epsilon}) \mp \frac{1}{2\pi\sqrt{\epsilon}}\sum_{m=1}^{\infty}[L_x\cos(2L_xm\sqrt{\epsilon}) + L_y\cos(2L_ym\sqrt{\epsilon})] \tag{B4}$$

$$\text{triangle} \to \widetilde{\rho}_{\mathrm{D,N}}(\epsilon) \ = \ \frac{A}{4\pi}\sum_{\mathbf{M}} J_0(L_{\mathbf{M}}\sqrt{\epsilon}) \mp \frac{3L}{4\pi\sqrt{\epsilon}}\sum_{m=1}^{\infty}\cos((3L/2)m\sqrt{\epsilon}) \tag{B5}$$

with double index $\mathbf{M} = (M_1, M_2)$ running over integer numbers, excluding from the sum the term $(M_1, M_2) = (0, 0)$, which indeed had given the area term in Weyl series. The length of periodic orbits are $L_{\mathbf{M}} = 2\sqrt{(M_1L_x)^2 + (M_2L_y)^2}$ for the rectangle, and $L_{\mathbf{M}} = \sqrt{3(M_1^2 + M_2^2 + M_1M_2)}L$ for the equilateral triangle.

We see that for both shapes, and both boundary conditions, the structure of the formulae are very similar. We have first to evaluate the integral of terms with J_0 function, that can be solved analytically

$$\int_0^\infty \mathrm{d}\epsilon\sqrt{\epsilon}K_1(2la\sqrt{\epsilon})J_0(L_{\mathbf{M}}\sqrt{\epsilon}) = \frac{l}{2a^3(l^2+(L_{\mathbf{M}}/2a)^2)^2} \tag{B6}$$

Using this into (B1) the resulting l sum can also be performed

$$\sum_{l=1}^{\infty}\frac{1}{(l^2+\alpha^2)^2} = \frac{2\pi^2\alpha^2+2\pi\alpha\sinh(\pi\alpha)\cosh(\pi\alpha)-\sinh^2(\pi\alpha)}{8\alpha^4\sinh^2(\pi\alpha)} = \frac{\pi}{4\alpha^3}-\frac{1}{2\alpha^4}+\mathcal{O}(\mathrm{e}^{-2\pi\alpha}) \tag{B7}$$

with $\alpha = L_{\mathbf{M}}/2a$. We used the approximation $\alpha \gg 1$, corresponding to the limit of small plate separation a (compared to the typical plate's size). The final contribution of the J_0 terms to the Casimir energy is

$$-\frac{A}{2\pi}\left(\frac{1}{4}\sum_{\mathbf{M}}\frac{1}{L_{\mathbf{M}}^3}-\frac{a}{\pi}\sum_{\mathbf{M}}\frac{1}{L_{\mathbf{M}}^4}\right) \tag{B8}$$

which is the same for TE and TM modes, and both shapes. As a function of plate separation a, there are a constant term plus a linear term on a.

For the terms in $\widetilde{\rho}$ with cosines, we have integrals of type

$$\int_0^\infty \mathrm{d}\epsilon K_1(2la\sqrt{\epsilon})\cos(Rm\sqrt{\epsilon}) = \frac{\pi l}{4a^2(l^2+(Rm/2a)^2)^{3/2}} \tag{B9}$$

with $R = 2L_x$ or $2L_y$ for the two terms in the rectangular billiard, and $R = 3L/2$ for the equilateral triangle. Now the sum over l can not be done analytically, but we give an approximation

$$\sum_{l=1}^{\infty}\frac{1}{(l^2+\alpha^2)^{3/2}} = \frac{1}{\alpha^2}-\frac{1}{2\alpha^3}+\mathcal{O}(\mathrm{e}^{-\alpha}) \tag{B10}$$

valid for $\alpha = Rm/2a \gg 1$. The sum over index m can be done in terms of Riemann Zeta function. Finally, the contribution of the cosine terms to the Casimir energy of TM modes (given by the Dirichlet density of states) is

$$\text{rectangle} \;\to\; \frac{\zeta(2)}{16\pi}\left(\frac{1}{L_x}+\frac{1}{L_y}\right)-\frac{\zeta(3)}{32\pi}\left(\frac{1}{L_x^2}+\frac{1}{L_y^2}\right)a \tag{B11}$$

$$\text{triangle} \;\to\; \frac{\zeta(2)}{6\pi L}-\frac{\zeta(3)}{9\pi L^2}a \tag{B12}$$

For TE modes the contribution has exactly the opposite sign. We see again a constant plus a linear term on plate separation a. We remark here that on semiclassical approximation ($\epsilon \to \infty$), usually terms coming from cosine in Eqs. B4 and B5 are ignored compared to the main terms from periodic orbit, and even the J_0 function is approximated by its asymptotic expression for big arguments. But due to the integration from low energies, we see that both J_0 and cosine terms give contributions of the same order on a. This is the reason why a general semiclassical approximation, only valid for high energies, will not be enough to compute the contributions to Casimir energy.

Collecting all terms we have the correcting part of the Casimir energy for the rectangle

$$\delta E_{\mathrm{D,N}}(a) \;=\; -\frac{L_xL_y}{8\pi}\sum_{\mathbf{M}}\frac{1}{L_{\mathbf{M}}^3}\pm\frac{\pi}{96}\left(\frac{1}{L_x}+\frac{1}{L_y}\right)+a\frac{L_xL_y}{2\pi^2}\sum_{\mathbf{M}}\frac{1}{L_{\mathbf{M}}^4}\mp a\frac{\zeta(3)}{32\pi}\left(\frac{1}{L_x^2}+\frac{1}{L_y^2}\right) \tag{B13}$$

and for the equilateral triangle

$$\delta E_{\mathrm{D,N}}(a) \;=\; -\frac{\sqrt{3}L^2}{32\pi}\sum_{\mathbf{M}}\frac{1}{L_{\mathbf{M}}^3}\pm\frac{\pi}{36L}+a\frac{\sqrt{3}L^2}{8\pi^2}\sum_{\mathbf{M}}\frac{1}{L_{\mathbf{M}}^4}\mp a\frac{\zeta(3)}{9\pi L^2}\;. \tag{B14}$$

Deriving with respect to a we finally obtain, up to exponentially small terms, the correcting part of the Casimir force

$$\text{rectangle} \;\rightarrow\; \delta F_{\rm D,N} = -\frac{L_x L_y}{2\pi^2}\sum_{\mathbf{M}}\frac{1}{L_{\mathbf{M}}^4} \pm \frac{\zeta(3)}{32\pi}\left(\frac{1}{L_x^2}+\frac{1}{L_y^2}\right) \tag{B15}$$

$$\text{triangle} \;\rightarrow\; \delta F_{\rm D,N} = -\frac{\sqrt{3}L^2}{8\pi^2}\sum_{\mathbf{M}}\frac{1}{L_{\mathbf{M}}^4} \pm \frac{\zeta(3)}{9\pi L^2}\ , \tag{B16}$$

which are constants.

Acknowledgments

The work of E.A., F.D.M. and D.A.W. was supported by UBA, CONICET and ANPCyT. The work of A.G.M. was supported by CNEA and CONICET.

[1] P. W. Milonni, it The Quantum Vacuum, Academic Press, San Diego, 1994; M. Bordag, U. Mohideen, and V. M. Mostepanenko, Phys. Rep. **353**, 1 (2001); K. A. Milton, *The Casimir Effect: Physical Manifestations of the Zero-Point Energy* (World Scientific, Singapore, 2001); S. Reynaud *et al.*, C. R. Acad. Sci. Paris **IV-2**, 1287 (2001); K. A. Milton, J. Phys. A: Math. Gen. **37**, R209 (2004); S.K. Lamoreaux, Rep. Prog. Phys. **68**, 201 (2005); M. Bordag, G.L. Klimchitskaya, U. Mohideen, and V. M. Mostepanenko, *Advances in the Casimir Effect*, Oxford University Press, Oxford, 2009.

[2] R. M. Cavalcanti, Phys. Rev. D **69**, 065015 (2004) [arXiv:quant-ph/0310184]; M. P. Hertzberg, R. L. Jaffe, M. Kardar and A. Scardicchio, Phys. Rev. Lett. **95**, 250402 (2005) [arXiv:quant-ph/0509071]; G. Barton, Phys. Rev. D **73**, 065018 (2006); S.A. Fulling and J.H. Wilson, Phys. Rev. A **76**, 012118 (2007); A. Edery, Phys. Rev. D **75**, 105012 (2007) [arXiv:hep-th/0610173]. X. Zhai, X. Li, Phys.Rev. D **76**, 047704 (2007); V.N. Marachevsky, J.Phys.A **41**, 164007 (2008); A. Edery and V. Marachevsky, Phys. Rev. D **78**, 025021 (2008) [arXiv:0805.4038 [hep-th]]; A. Edery and I. MacDonald, JHEP **0709**, 005 (2007) [arXiv:0708.0392 [hep-th]].

[3] V. N. Marachevsky, Phys. Rev. D **75**, 085019 (2007) [arXiv:hep-th/0703158].

[4] A. Rodriguez, M. Ibanescu, D. Iannuzzi, F. Capasso, J. D. Joannopoulos, and S.G. Johnson, Phys. Rev. Lett. **99**, 080401 (2007).

[5] O. Bohigas, M.-J. Gianonni, and C. Schmit, Phys. Rev. Lett. **52**, 1 (1984).

[6] M. V. Berry and M. Tabor, Proc. Roy. Soc. London **A 356**, 375 (1977)

[7] H. J. Stockmann, Quantum Chaos: An Introduction (Cambridge U. Press,Cambridge, 1999). M. C. Gutzwiller, Chaos in Classical and Quantum Mechanics (Springer Verlag, New York, 1990).

[8] M. P. Hertzberg, R. L. Jaffe, M. Kardar and A. Scardicchio, Phys. Rev. D **76**, 045016 (2007) [arXiv:0705.0139 [quant-ph]].

[9] K. Kirsten and S. A. Fulling, Phys. Rev. D **79**, 065019 (2009) [arXiv:0901.1902 [hep-th]].

[10] M.G. Lamé, *"Leçons sur la théorie mathématique de l'élasticité des corps solides"* (Bachelier, Paris, 1852), 57, p.131.

[11] M. Schaden and L. Spruch, Phys. Rev. A **58**, 935 (1998); F. D. Mazzitelli,1 M. J. Sánchez, N. N. Scoccola, and J. von Stecher, Phys. Rev. A **67**, 013807 (2003); M. Schaden, arXiv:1006.3262 [quant-ph].

[12] E. Vergini and M. Saraceno Phys. Rev. E **52**, 2204 (1995).

[13] A. H. Barnett and T. Betcke, CHAOS, **17**, 043123 (2007); and A.H. Barnett ArXiv:math-ph/0512030v2.

[14] E. Alvarez and F. D. Mazzitelli, Phys. Rev. D **79**, 045019 (2009) [arXiv:0901.2641 [hep-th]].

[15] See for instance K. A. Milton, *The Casimir Effect: Physical Manifestations of the Zero-Point Energy* (World Scientific, Singapore, 2001), Chapter 2.

[16] M. Brack and R.K. Bhaduri, *"Semiclassical Physics"*, Adison-Wesley publishing Company (1997), Ch.3.

[17] J.R. Kuttler and V.G. Sigillito, SIAM Review **26**, 163 (1984).

[18] L.A. Bunimovich, Commun. Math. Phys. **65**, 295 (1979).

[19] A. Barnett, http://www.math.dartmouth.edu/∼ahb/qugrs_n62076.Es .

[20] T. Prosen, Phys. Lett. A **233** 323 (1997).

[21] A. H. Barnett, Comm. Pure Appl. Math., **59**, 1457-1488 (2006).

[22] J.V. Villadsen and E. Stewart, Chem. Engng. Sci. **22**, 1483 (1967); T. Betcke and L.N. Trefethen, SIAM Review **47**, 469 (2005)C.J.S. Alves and P.R.S. Antunes, CMC **2**, 251 (2005); D. Cohen, N. Lepore and E.J. Heller, J. Phys. A: Math. Gen. **37**, 2139 (2004); P. Amore, J. Math. Phys. **51**, 052105 (2010)

[23] F.C. Lombardo, F.D. Mazzitelli, P.I. Villar, and M. Vázquez, Phys. Rev. D**80**, 0605018 (2009); F.C. Lombardo, F.D. Mazzitelli, P.I. Villar, *Proceedings of the Ninth Conference on Quantum Field Theory Under the Influence of External Conditions*, edited by K.A. Milton and M. Bordag,World Scientific, Singapore (2010).